

ChemComm

Accepted Manuscript



This is an *Accepted Manuscript*, which has been through the Royal Society of Chemistry peer review process and has been accepted for publication.

Accepted Manuscripts are published online shortly after acceptance, before technical editing, formatting and proof reading. Using this free service, authors can make their results available to the community, in citable form, before we publish the edited article. We will replace this *Accepted Manuscript* with the edited and formatted *Advance Article* as soon as it is available.

You can find more information about *Accepted Manuscripts* in the [Information for Authors](#).

Please note that technical editing may introduce minor changes to the text and/or graphics, which may alter content. The journal's standard [Terms & Conditions](#) and the [Ethical guidelines](#) still apply. In no event shall the Royal Society of Chemistry be held responsible for any errors or omissions in this *Accepted Manuscript* or any consequences arising from the use of any information it contains.

Cite this: DOI: 10.1039/c0xx00000x

www.rsc.org/xxxxxx

ARTICLE TYPE

Integration of bacteriorhodopsin with upconversion nanoparticles for NIR-triggered photoelectrical response

Zhisong Lu, *^{a,b,c} Jing Wang,^{a,b,c} Xiutao Xiang,^{a,b,c} Rui Li,^d Yan Qiao^{a,b,c} and Chang Ming Li*^{a,b,c}

Received (in XXX, XXX) Xth XXXXXXXXXX 20XX, Accepted Xth XXXXXXXXXX 20XX

5 DOI: 10.1039/b000000x

Transient spikes from the bacteriorhodopsin (bR) photocycle are triggered with NIR irradiation for the first time by integrating bR with upconversion nanoparticles. This work may open new horizons for the bR applications in the IR wavelength range.

Bacteriorhodopsin (bR) is a retinal-containing chromo-protein embedding in purple membrane (PM) of *Halobacterium salinaru*.¹ It has two configurations: light- and dark-adopted forms that can switch from one to another under light irradiation. bR in the former one comprises all-trans-retinal with a maximum absorption at 568 nm.² When exposure to light with appropriate wavelengths, it undergoes a series of photochemical reactions, in which the all-trans-retinal isomerizes to 13-cis-retinal, sequentially forming several dark-adopted “J, K, L, M and N” intermediates. After further experiencing the “O” intermediate with the retinal re-isomerizing to all-trans, the bR recycles back to its initial light-adapted configuration. A transient photocurrent is generated by the proton transmembrane movement during the photocycle.³ Due to its photoresponse, bR has been regarded as one of the most promising native biomaterials for applications in optical electronics,⁴ optical storage,⁵ information processing,⁶ nonlinear optics⁷ and solar conversion.⁸

As advances of nanotechnology, nanomaterials with unique functions have been incorporated with bR to achieve photoelectric responses with either enhanced amplitude or novel pattern.⁷⁻⁹ Our group has constructed a hybrid bR and CdTe quantum dots (QDs) biosystem, in which QDs serve as internal nanoscale light sources to generate a stationary photocurrent differently from the transient spikes.¹⁰ Since the plasmonic field can cause alteration of both the retinal photoisomerization and the proton pump process, the stationary photocurrent has also been observed by mixing bR with plasmonic nanoparticles such as gold and silver nanoparticles.¹¹ Besides the novel photoelectric current pattern, QDs have been used to enhance the transient photocurrent of bR via the Förster resonance energy transfer (FRET) from QDs to bR.¹² In our previous work, bR was incorporated in a multilayered WO₃•H₂O nanocrystals/PVA membrane, in which the photoelectric response of bR was greatly enhanced by the spillover effect of WO₃•H₂O nanocrystals.⁹ Since bR can absorb visible light and transform it into electricity, its combination with semiconducting nanomaterials for solar energy conversion has aroused tremendous interest in recent years. bR has been immobilized on TiO₂ nanocrystals to fabricate

a dye sensitized solar cell.¹³ It can also be used to functionalize TiO₂ nanotubes for photoelectrochemical water splitting.¹⁴

Although the extraordinary properties have been achieved by integrating bR with various nanomaterials, the intrinsic visible light absorption of bR cannot be changed because of its retinal-containing chromo-protein nature. Infra-red (IR) is an important part of the solar electromagnetic radiation that reaches the earth.¹⁵ In order to enhance the solar energy conversion efficiency of the bR based system, it is highly desirable to develop a strategy that can tune the bR-sensitive wavelengths to IR range. However, there is no report on a bR incorporation system with IR-triggered photoresponse up to date. Upconversion nanoparticles (UCNPs), particularly lanthanide-doped nanocrystals, which emit high energy photons under excitation by the near-infrared (NIR) light, have been extensively studied as very promising fluorescent materials for biological labeling,¹⁶ imaging¹⁷ and therapeutics¹⁸. NaYF₄:Yb,Er nanocrystal is one of the most efficient 980 nm NIR to visible (bright green) up-conversion phosphors.¹⁹ In this study, its upconversion capability was combined with bR-initiated photocycle to fabricate a system with NIR-triggered photoelectric responses.

PM was isolated from *Halobacterium halobium* S9 strain according to our previous works²⁰ and further characterized with UV-visible spectroscopy and atomic force microscopy (AFM). Water-soluble polyethylenimine (PEI)-modified NaYF₄:Yb (20%),Er (2%) nanocrystals were synthesized with a one-pot hydrothermal method according to Wang's route²¹. bR and PEI-UCNPs suspensions were dropped on a ITO slide (0.8 cm×0.8 cm) and a IRCF (Cut-off wavelength range 700-1100nm, 0.8 cm×0.8 cm), respectively, followed by drying at 30 °C for 1 hr. The ITO and the IRCF were mounted together back to back. A U-shaped groove was attached between the ITO/IRCF stacking electrode (working electrode) and a platinum sheet electrode (counter electrode) to form a closed container for loading of the electrolyte solution. The experimental details are described in the electronic supplementary information (ESI).

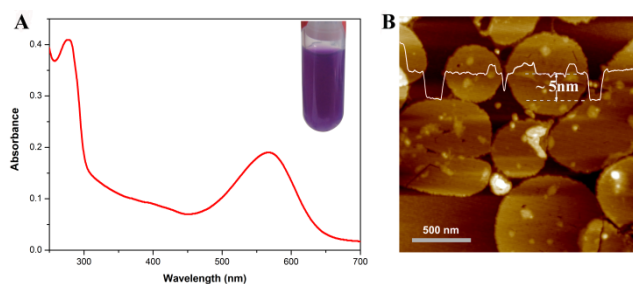


Fig. 1 (A) UV-Vis spectrum of isolated bR-PM. Inset: picture of bR-PM suspension; (B) AFM image of isolated purple membrane patches.

The PM suspension has a characteristic maximum absorbance 5 at 570 nm, which could be assigned to the absorption of bR in its ground state (Fig. 1A).²⁰ The concentration of bR is calculated to be 1.65 mg/mL based on the Lambert-Beer's law. AFM image shows PM patches on the mica surface with a thickness of ~5 nm (Fig. 1B), which is in good agreement with the topology and 10 thickness of PM observed in previous investigations.^{1,20} The results indicate that the quality of the bR can meet the requirements of following experiments.

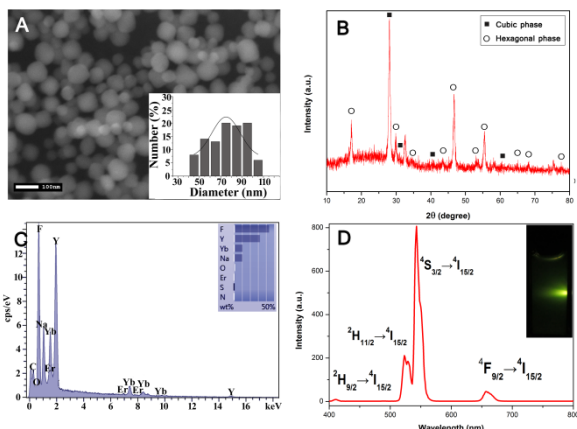


Fig. 2 (A) FESEM image of PEI-NaYF₄:Yb,Er. Inset: size distribution of PEI-NaYF₄:Yb,Er; (B) XRD patterns for the as-prepared PEI-NaYF₄:Yb,Er; (C) EDX spectrum of PEI-NaYF₄:Yb,Er; (D) PL emission spectra and digital camera image of the PEI-NaYF₄:Yb,Er under the irradiation of a 980 nm laser (2000 mW/cm²).

NaYF₄:Yb,Er nanocrystal with efficient upconversion 20 capability is another critical component of the designed system. The morphology of the prepared NaYF₄:Yb,Er UCNPs was examined with field emission-scanning electron microscope (FESEM) (Fig. 2A). Monodispersed nanocrystals exhibit spherical shapes with a size range from 40 to 110 nm, which are 25 consistent with the PEI-functionalized NaYF₄:Yb,Er synthesized using the same approach.²¹ The X-ray powder diffraction (XRD) pattern shows well-defined peaks, indicating high crystallinity of the products, and the peak positions match well with both hexagonal phase (JCPDS standard card 28-1192) and cubic phase 30 (JCPDS standard card 77-2042) of NaYF₄:Yb,Er (Fig. 2B). The energy dispersive X-ray analysis (EDS) spectrum confirms the existence of fluorine, sodium, ytterbium and yttrium atoms in the crystals. Furthermore, doping of erbium in the UCNPs could also be verified by the spectrum (Fig. 2C). The upconversion- 35 luminescence spectrum of the UCNPs under 980 nm excitation (2000 mW/cm²) shows three emission peaks at 524, 543, and 658

nm for PEI-NaYF₄:Yb,Er UCNPs, corresponding to the transitions ²H_{11/2}→⁴I_{15/2}, ⁴S_{3/2}→⁴I_{15/2} and ⁴F_{9/2}→⁴I_{15/2}, respectively, for the Er³⁺ (Fig. 2D).²² The strongest emission of 40 PEI-NaYF₄:Yb,Er UCNPs is in a wavelength range of 520 to 580 nm, which matches the maximum absorption of bR. Thus, the strong green photoluminescence from the UCNPs under the NIR excitation has the potential to trigger bR photoresponses.

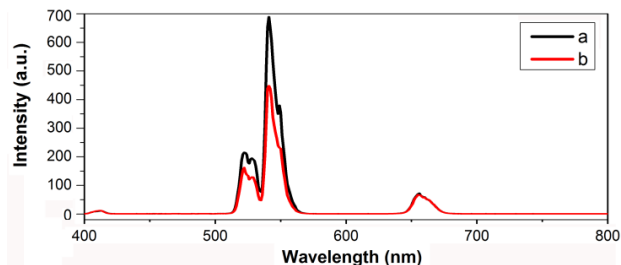


Fig. 3 (a) PL emission spectra of PEI-NaYF₄:Yb,Er through blank ITO; (b) PL emission spectra of PEI-NaYF₄:Yb,Er through the ITO attached with bR layer under the irradiation of a 980 nm laser (2000 mW/cm²).

A conventional bR-based photo-harvesting electrode was 50 fabricated by immobilizing a layer of bR-embedded PM on the indium-tin-oxide (ITO)-glass surface. Due to a slight change of the local temperature direct IR irradiation on the bare electrode surface induces a very significant electrical response, which overlaps the transient spikes from bR (Fig. S1). Thus, UCNP cannot be directly mixed with bR to fabricate the device. To 55 avoid the electrical interference from IR, a UCNPs-coated IR cut filter (IRCF, cut-off wavelength range 700-1100 nm) was stacked with a PM-ITO glass electrode back to back to efficiently remove transmitted NIR for the upconversion-luminescence measurement. For clear comparison, a UCNPs-coated IRCF attached with a bare 60 ITO-glass electrode was used as a control. Under 980 nm excitation (2000 mW/cm²), the emission peaks of UCNPs can be observed on both samples, suggesting that the use of IRCF does not cut off the emission of UCNPs. In comparison to the control sample, bR immobilized on ITO-glass leads to a significant 65 reduction of luminescence in the wavelength range of 520-580 nm without affecting the emission peak at 658 nm (Fig. 3). Because the PM and the UCNP layers are spaced by an ITO glass and an IRCF filter, FRET cannot occur in the UCNP/IRCF/ITO/PM system due to the large distance between 70 the nanoparticles and the bR molecules. As shown in Fig. 1A and Fig. 2D, the emission of UCNPs from 520 to 580 nm overlaps the absorption spectrum of bR. Therefore, the phenomenon can be reasonably explained by re-absorption of the UCNP emission by bR. Based on the results, the photocycle of bR is very likely to be 75 triggered by the green light emitted from the excited UCNPs.

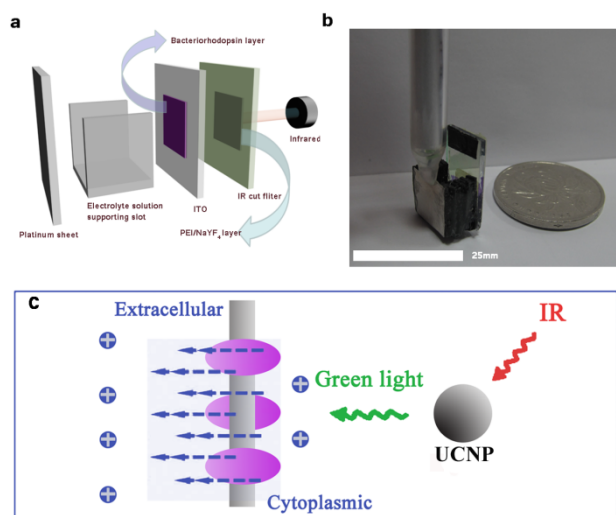


Fig. 4 (a) Schematic of photoelectric responses measurement device; (b) Image of the device in practical experiment; (c) The light energy transfer from UCNPs to bR-PM.

5 To monitor the NIR-triggered photoelectrical response, a device was constructed as illustrated in Fig. 4. The PM-ITO/IRCF-UCNPs stacking electrode mentioned above was used as the working electrode while employing a platinum sheet as the counter electrode. A U-shape rubble groove was stuck between
10 two electrodes to load electrolyte solution. CHI 660E potentiostat (Shanghai Chenhua Instrumental Cooperation Ltd., China) was used to quantify the photoelectric response with amperometric measurements at the open circuit potential. Bare ITO electrode has no response to a green light irradiation (535 ~ 600 nm). After
15 bR immobilization, typical photocurrent profiles can be observed under the green light, showing that the activity of the isolated bR-embedded PM is maintained. A bare IRCF attached on the PM-coated ITO electrode has no obvious effect on its performance (Fig. 5a). A stacking electrode without the PM coating layer was
20 tested to eliminate the possible interference from UCNPs under the 980 nm excitation. Fig. 5b shows that the stacking electrode without bR has no response to NIR light. However, transient photocurrent spikes are found for the device with PM-ITO/IRCF-UCNPs stacking electrode under NIR irradiation, indicating that
25 the green light converted by NIR-excited UCNPs successfully triggers the proton pump and initiates the photocycle of bR (Fig. 5b). The calculated energy conversion efficiency of the device was about 10⁻¹¹% in terms of the experimental results, which is quite low in comparison to ~0.1% reported for a bR-ZnO
30 nanostructured photoelectrode under the AM1.5 irradiation.¹³ Some strategies may improve the device efficiency. UCNPs with better quantum efficiency may be utilized in the system to generate high-intensity green light under the IR irradiation for enhancement of the energy efficiency. The thicknesses of the ITO
35 and IRCF glasses could be reduced to facilitate the re-absorption of UCNPs emission by bR. Alternatively, orientation of PM could be optimized to enhance the light-triggered electrical signals, or a short distance between the photo-electrode and platinum electrode may be used to decrease the internal resistance
40 of the device. These optimization works are on-going in the authors' lab. Although the density of the photocurrent was relatively weaker than that of the photocurrent directly generated

by green light source excitation, it still clearly proves that IR triggered electrical response of bR can be realized by integrating
45 bR with UCNPs.

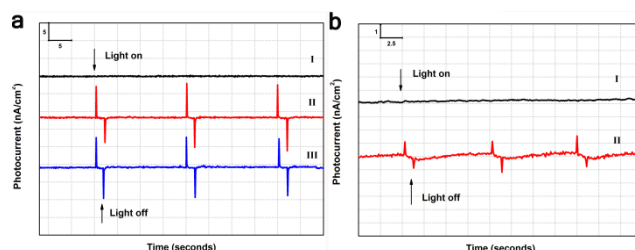


Fig. 5 (a) Photocurrent of (I) blank ITO, (II) ITO with bR-PM layer, (III) ITO with bR-PM layer and add a IRCF illuminated by green light (535~600nm); (b) Photocurrent of (I) blank ITO, (II) ITO with bR-PM layer under the irradiation of 980nm IR (2000 mW/cm²) through a PEI-NaYF₄: Yb, Er attached IR cut filter.

In brief, a novel device by integrating bR with UCNPs was fabricated to produce NIR-triggered photoelectrical responses that were different from conventional visible-light stimulating
55 ones. The re-absorption of NIR-excited UCNPs luminescence by bR molecules can be used to explain the phenomenon. This work may open new horizons for the bR applications in the IR wavelength range.

This work is financially supported by National Program on
60 Key Basic Research Project of China (973 Program) under contract No.2013CB127804, National Natural Science Foundation of China (Grant No. 21103059), Chongqing Key Laboratory for Advanced Materials and Technologies of Clean Energies under cstc2011pt-sy90001, Start-up grant under
65 SWU111071 from Southwest University and Chongqing Science and Technology Commission under cstc2012gjhz90002 (Chongqing, China). Z. S. Lu would like to thank the supports by the Specialized Research Fund for the Doctoral Program of Higher Education (RFDP) (Grant No. 20130182120025), Young
70 Core Teacher Program of the Municipal Higher Educational Institution of Chongqing and Chongqing Key Natural Science Foundation (cstc2012jjA1137).

Notes and references

- 75 a Chongqing Key Laboratory for Advanced Materials & Technologies of Clean Energies, 1 Tiansheng Road, Chongqing 400715, P. R. China
b Institute for Clean Energy & Advanced Materials, Faculty of Materials and Energy, Southwest University, 1 Tiansheng Road,
80 Chongqing 400715, P. R. China.
c Chongqing Engineering Research Center for Rapid Diagnosis of Fatal Diseases, 1 Tiansheng Road, Chongqing 400715, P. R. China. Fax: +86-23-68254969; Tel: +86-23-68254727; E-mail: ecml@swu.edu.cn or zslu@swu.edu.cn
85 d Section of Environmental Biomedicine, Hubei Key Laboratory of Genetic Regulation and Integrative Biology, College of Life Sciences, Central China Normal University, Wuhan 430079, P. R. China
† Electronic Supplementary Information (ESI) available: [details
90 of any supplementary information available should be included here]. See DOI: 10.1039/b000000x
1 N. Hampp, *Chem. Rev.*, 2000, **100**, 1755.
2 (a) M. Rehorek and M. P. Heyn, *Biochemistry*, 1979, **18**,

- 4977; (b) B. Becher, F. Tokunaga and T. G. Ebrey, *Biochemistry*, 1978, **17**, 2293.
- 3 (a) B. Robertson and E. P. Lukashev, *Biophys. journal*, 1995, **68**, 1507; (b) J.-p. Wang, L. Song, S.-k. Yoo and M. A. El-Sayed, *J. Phys. Chem. B*, 1997, **101**, 10599; (c) J.-P. Wang, S.-K. Yoo, L. Song and M. A. El-Sayed, *J. Phys. Chem. B*, 1997, **101**, 3420.
- 5 4 (a) L. Fábrián, E. K. Wolff, L. Oroszi, P. Ormos and A. Dér, *Appl. Phys. Lett.*, 2010, **97**, 023305; (b) S. Roy, M. Prasad, J. Topolancik and F. Vollmer, *J. Appl. Phys.*, 2010, **107**, 053115.
- 5 (a) M. Imhof, D. Rhinow and N. Hampp, *Appl. Phys. Lett.*, 2014, **104**, 081921; (b) X. Yu, B. Yao, M. Lei, P. Gao and B. Ma, *J. Modern Opt.*, 2013, **60**, 309.
- 15 6 N. Burykin, D. Stepanchikov, T. Dyukova, A. Savchuk, S. Balashov and E. Korchemskaya, *Mol. Cryst. Liquid Cryst.*, 2011, **535**, 140.
- 7 A. Rakovich, I. Nabiev, A. Sukhanova, V. Lesnyak, N. Gaponik, Y. P. Rakovich and J. F. Donegan, *ACS nano*, 2013, **7**, 2154.
- 20 8 C.-W. Yen, S. C. Hayden, E. C. Dreaden, P. Szymanski and M. A. El-Sayed, *Nano lett.*, 2011, **11**, 3821.
- 9 C. MingáLi, *Chem. Commun.s*, 2010, **46**, 689.
- 10 R. Li, C. M. Li, H. Bao, Q. Bao and V. S. Lee, *Appl. Physics Lett.*, 2007, **91**, 223901.
- 25 11 C.-W. Yen, L.-K. Chu and M. A. El-Sayed, *J. Am. Chem. Soc.*, 2010, **132**, 7250.
- 12 A. Rakovich, A. Sukhanova, N. Bouchonville, E. Lukashev, V. Oleinikov, M. Artemyev, V. Lesnyak, N. Gaponik, M. Molinari and M. Troyon, *Nano lett.*, 2010, **10**, 2640.
- 30 13 A. Molaeirad and N. Rezaeian, *Biotechnol. Appl. Biochem.*, 2014, doi: 10.1002/bab.1294.
- 14 N. K. Allam, C.-W. Yen, R. D. Near and M. A. El-Sayed, *Energy Environ. Sci.*, 2011, **4**, 2909.
- 35 15 S. M. Chaurasiya, S. Kirpekar and A. R. Arankalle, in *Innovative Design, Analysis and Development Practices in Aerospace and Automotive Engineering*, Springer, 2014, pp. 269-275.
- 16 (a) D. K. Chatterjee, A. J. Rufaihah and Y. Zhang, *Biomaterials*, 2008, **29**, 937; (b) Q. Dou, N. M. Idris and Y. Zhang, *Biomaterials*, 2013, **34**, 1722; (c) W. Zhang, B. Peng, F. Tian, W. Qin and X. Qian, *Anal. Chem.*, 2013, **86**, 482.
- 40 17 (a) Q. Liu, Y. Sun, T. Yang, W. Feng, C. Li and F. Li, *J. Am. Chem. Soc.*, 2011, **133**, 17122; (b) L. L. Li, R. Zhang, L. Yin, K. Zheng, W. Qin, P. R. Selvin and Y. Lu, *Angew. Chemie Internat. Ed.*, 2012, **51**, 6121; (c) G. Chen, H. Qiu, P. N. Prasad and X. Chen, *Chem. Rev.*, 2014.
- 45 18 (a) C. Wang, L. Cheng and Z. Liu, *Biomaterials*, 2011, **32**, 1110; (b) F. Wang, D. Banerjee, Y. Liu, X. Chen and X. Liu, *Analyst*, 2010, **135**, 1839; (c) Q. Chen, C. Wang, L. Cheng, W. He, Z. Cheng and Z. Liu, *Biomaterials*, 2014, **35**, 2915.
- 50 19 (a) G. Tian, Z. Gu, L. Zhou, W. Yin, X. Liu, L. Yan, S. Jin, W. Ren, G. Xing and S. Li, *Adv. Mater.*, 2012, **24**, 1226; (b) M. Haase and H. Schäfer, *Angew. Chemie Internat. Ed.*, 2011, **50**, 5808.
- 55 20 (a) K. Edman, P. Nollert, A. Royant, H. Belrhali, E. Pebay-Peyroula, J. Hajdu, R. Neutze and E. M. Landau, *Nature*, 1999, **401**, 822; (b) R. Li, X. Cui, W. Hu, Z. Lu and C. M. Li, *J. Colloid Interf. Sci.*, 2010, **344**, 150.
- 60 21 Y. Wang, P. Shen, C. Li, Y. Wang and Z. Liu, *Anal. Chem.*, 2012, **84**, 1466.
- 22 C. Liu, H. Wang, X. Li and D. Chen, *J. Mater. Chem.*, 2009, **19**, 3546.